Int. J. Heat Mass Transfer. Vol. 30, No. 10, pp. 2125–2136, 1987
Printed in Great Britain

0017–9310/87 $3.00 + 0.00

Radial mass flow in electrohydrodynamically-enhanced forced heat transfer in tubes

JOSÉ L. FERNÁNDEZ and ROBERT POULTER
Department of Mechanical Engineering, University of Bristol, Bristol, U.K.

(*Received* 25 *March* 1986 *and in final form* 17 *March* 1987)

Abstract—Experimental results of an electrohydrodynamically-enhanced oil heater of annular cross-section are presented. When a high d.c. voltage (typically 30 kV) was applied across the annular gap, it induced a very strong radial motion of the fluid resulting in a heat transfer increase of more than 20 fold over the fully-developed laminar flow, yet the pressure drop only increased 3 fold. The electrohydrodynamically-enhanced Nusselt number correlates well with electrical current passed, which is typically a few millionths of an ampere per metre of tube.

1. INTRODUCTION

VARIOUS studies in the field of electrohydrodynamics (EHD) show that the application of an electrostatic potential to a dielectric liquid flowing in a duct can improve the rate of heat exchange between the duct wall and the fluid [1]. Particularly in laminar flow in annular tubes, EHD forces are seen to induce a complex secondary flow within the main stream that results in an increase in the heat exchange rate of up to 2000%, typically, depending on characteristics of the fluid. This is attained with a typical EHD power consumption of about 0.05% of the enhanced heat transport rate [2, 3].

A complete understanding of the physical mechanisms of EHD is not in view and, therefore, the utilization of this technique to reduce the size and cost of industrial heat exchangers is still subject to detailed review. Recent work concerning the onset of instability in a liquid layer between planar electrodes (i.e. refs. [4–7]), may eventually yield the necessary theoretical background for the reduction of heat and mass transfer enhancement. From the limited experimental evidence that has been gathered so far, mostly concerning the EHD enhancement of laminar flow of dielectric oil in tubes, various empirical notions have been derived. It is the purpose of this paper to disclose some of the most relevant results in this field, previously unpublished, arising from the work at Bristol since 1972.

2. EHD-INDUCED RADIAL FLOW

The preferred method of establishing an electrostatic field in these experiments, introduces a thin wire along the centre of the tube, which, connected to a high-voltage d.c. source, imposes an electrostatic field within the tube flow, divergent in nature, with a high voltage gradient at the inner electrode surface, the outer tube wall being electrically earthed.

If the pumped fluid is dielectric, high electric stresses can be achieved, of the order of 10^6 V m^{-1}, before electrical breakdown (sparking) occurs. According to the fluid type and purity, a microcurrent typically of the order of 1 μA per metre of electrode at high voltage (30 kV) will thus be established between the inner electrode and the outer tube.

In order to visualize the EHD effect, a thin slice of a tube was sandwiched between transparent plates. Transformer oil was used as the working liquid and small polystyrene beads, of similar density and electrical properties, were used as tracers. A well defined, radial flow pattern arises as an electrostatic field is imposed. The thin aspect ratio of the experimental device precludes three-dimensional motions; the leaf-pattern motion (Fig. 1) was observed whether or not a thermal gradient was established, indicating that continuous work could be done by the EHD effect even in the absence of heat transfer. The circulation pattern was observed to prevail at all voltages, and the apparent velocities, along the out-flowing streamers, were seen to increase with voltage. Electric current also increased with voltage. The intensity of the motion and the level of current, at constant voltage, were higher with negative than with positive polarity. Similar results were obtained in tests with other liquids (carbon tetrachloride, ether, refrigerant 113, toluene, diacetone alcohol, benzene and xylene).

Further experiments were performed in visualization cells with an axial dimension of several diameters, effectively removing the constraint on axial motion. A semi-transparent metallic coating on the inside of glass and perspex tubes retained the possibility of visual observation while an electrical grounding was supplied. When energized, motions were again observed in the liquid, although now 'leaf-pattern' cells were seen to appear at various axial positions, unlike the planar cell pattern observed in the smaller device. The motions remained predominantly in the radial plane. When a temperature gradient was established

NOMENCLATURE

b	ion mobility
c_p	specific heat
c	momentum flux parameter defined in equation (4)
D	source strength defined in equation (5)
$\mathbf{E}$	electric field
$\mathbf{f}$	body force per unit volume
f	Fanning friction factor
g	gravitational acceleration
h	heat transfer coefficient
h'	heat transfer coefficient with applied voltage
h_0	heat transfer coefficient without applied voltage
i	electric current
k	thermal conductivity
M_r	radial mass flow
M_r''	radial momentum flux
$\dot{m}$	axial mass flow
n	voltage–current proportionality exponent
Nu	dimensionless Nusselt number
Pr	dimensionless Prandtl number
p	pressure
Δp	axial pressure drop
$\Delta p'$	axial pressure drop with applied voltage
Δp_0	axial pressure drop without applied voltage
Δp_{iso}	axial pressure drop, isothermal
Δp_{ht}	axial pressure drop with heat transfer
q	electric charge density
R	radius at a boundary
Re	dimensionless Reynolds number
r	radius, radial coordinate
T	temperature
ΔT	temperature change or temperature difference
t	time
u	velocity
v	voltage
z	axial coordinate.

Greek symbols

α	radial dimensionless Reynolds number
β	thermal expansion coefficient
γ	kinematic viscosity
ε	liquid electrical permittivity
θ	circumferential coordinate
λ	ratio of tube/electrode diameters
μ	dynamic viscosity
ρ	mass density.

Subscripts

0	free space
1	electrode
2	tube
b	bulk fluid
e	electrostatic
i	ion, charged species
in	conditions at test tube inlet
r	radius
s	surface
out	conditions at test tube outlet
z	axial position
θ	circumferential position.

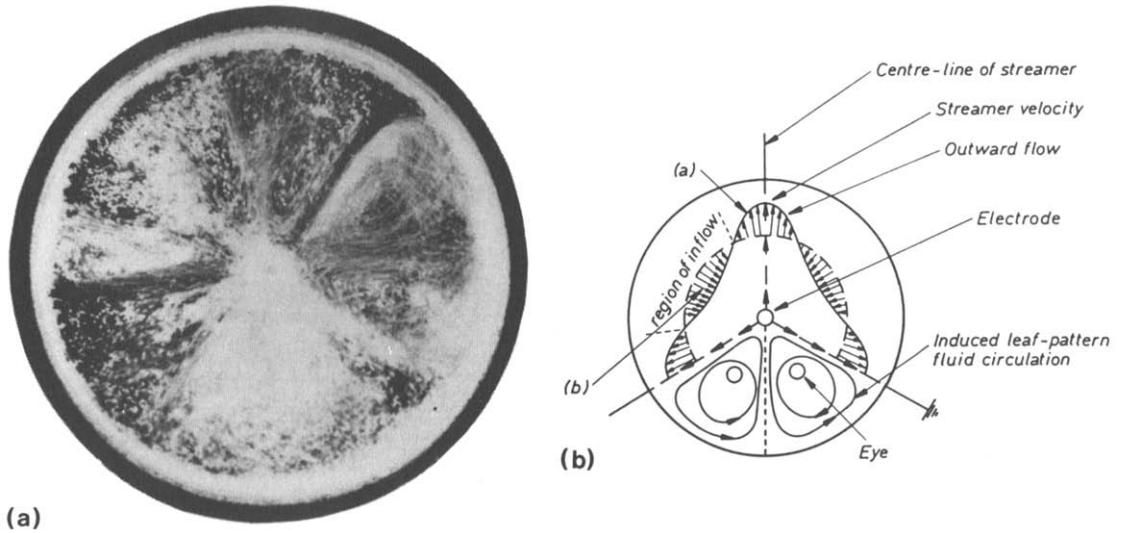

FIG. 1. (a) Streak photograph of electroconvective leaf pattern ($\lambda = 20, v = 30$ kV negative). (b) Distribution of radial velocity u, at $R_1 < r < R_2$.

on these longer devices, no major change in the motion pattern was perceived. Still, it was seen that at higher oil temperature (and therefore at lower viscosity) the motion and the current were stronger, at constant voltage, than at lower oil temperature.

The leaf-pattern motions previously described have not yet been observed when an axial flow is imposed. Undoubtedly, the resulting three-dimensional flow will prove to be extremely complex. However, the preceding results enlighten the knowledge in the field in two respects: (a) EHD produces the motion of liquid along streamers, and (b) of the various EHD forces capable of destabilizing a fluid, the one primarily responsible for the observed effect seems to be of electrophoretic nature, i.e. current dependent. The use of charge injection offers the possibility of continuous charge creation and annihilation within a fluid cell, enabling continuous work to be done.

3. A RADIAL MOMENTUM TRANSFER MODEL

The flow of a fluid, having a Newtonian character, subject to the effect of an electric field-induced force, can be described by the adequate equations for the conservation of mass, momentum and energy presented elsewhere (see, e.g. refs. [9, 10]).

Consider now a concentric tube arrangement containing an electrically stressed dielectric fluid of relative permittivity ε. Assuming that the conduction current is small so that the resultant space charge will not cause an appreciable distortion of the electric field (purely electrostatic case), we can write

$$\nabla \cdot \mathbf{E} = \frac{q}{\varepsilon} = 0 = -\nabla^2 v. \tag{1}$$

Given that the velocity of charged species in the host fluid is

$$u_i = -bE \tag{2}$$

then it can be shown that

$$u_i = \frac{bv_i}{r \ln \lambda} \tag{3}$$

where λ is the tube radius ratio. It is likely that this equation represents both the velocity of the charged species and of the host fluid in the inner regions of the annulus, since the Reynolds number for the charged species is low [8]; however, it will not be applicable to the fluid at the boundaries, where physical constraints demand that the fluid be at rest.

From continuity considerations in the two-dimensional geometry of Fig. 1, it can be seen that the point values of u_r along a streamer are substantially larger than any value of u_θ. It is now proposed that the local velocity of the streamer be taken as proportional to $1/r$ only, away from the immediate neighbourhood of the boundaries. The maximum value of the velocity u_r would be along a streamer, see Fig. 1. Correspondingly, relative values of u_θ are bound to be small in the model proposed.

The outward flow along each streamer will induce two recirculating cells, or 'leaves', mostly symmetrical about the streamer. This symmetrical flow represents an outward flow of momentum, a fact that is consistent with the notion that the electric work being done on the fluid arises from a unidirectional current flow. The radial momentum flux can be found as

$$M_r'' = c/r \tag{4}$$

where

$$c = \rho b^2 v_1^2 \int_0^{2\pi} f^2(\theta)\, \mathrm{d}\theta/(\ln \lambda)^2$$

and $f(\theta)$ is a moderating function modelling the features of the flow in Fig. 1. It will incorporate the necessary asymmetry to result in a net momentum transfer (for u_r outwards will be greater than inwards), at the same time ensuring that no net mass transfer is possible.

Since the quantity c is independent of r, this approach results in a one-dimensional equation for the momentum flux.

Since continuity considerations applied to the radial flow can be expressed as $M_r = 2\pi r u_r$, then, for a constant value of the radial mass flow rate M_r, the radial velocity becomes

$$u_r = D/r \tag{5}$$

where D is termed the 'source strength', so that the momentum flux will be

$$M_r'' = \int_0^{2\pi} \rho \frac{D^2}{r^2} r\, \mathrm{d}\theta = 2\pi\rho \frac{D^2}{r}. \tag{6}$$

Since equations (4) and (6) are meant to be equivalent, then $D = (c/2\pi\rho)^{1/2}$.

It can also be shown that u_z is a function of radius only. If the Navier–Stokes equation is solved for the radial direction and equation (5) is substituted, it can be shown that

$$\frac{\partial p}{\partial r} = \rho \frac{D^2}{r^3}. \tag{7}$$

This expression indicates that the gradient of pressure diminishes very rapidly in the outward direction, which agrees well with the theory of the 'corona wind'.

Substituting equation (6) in the equation of motion in the axial direction, a solution is found of the form

$$\frac{1}{\mu}\frac{\partial p}{\partial z} = \frac{\partial^2 u_z}{\partial r^2} + (1-\alpha)\frac{1}{r}\frac{\partial u_z}{\partial r} \tag{8}$$

where $\alpha = \rho D/\mu$, a 'radial Reynolds number'. For the no electric-flow condition, equation (8) is seen to reduce to the familiar Hagen–Poiseuille flow in an annulus.

The integration of equation (8) with the usual boundary conditions yields the structure of the axial velocity field u_z and its dependency on the EHD effect represented by α. It can be seen that there is an increased distortion in the velocity profile when α is increased, resulting in an increased pressure drop.

In the presence of heat transfer, the above results would not apply readily since buoyancy forces would be present, some contribution due to dielectrophoresis would have to be accounted for, and equation (1) would be invalid in the presence of a temperature gradient due to the temperature dependence of ε. The problem is further complicated by the high viscosity/temperature sensitivity of the oil used in this work.

A more elaborate model to account for these variations cannot be justified with the present unsatisfactory knowledge of EHD interaction, and is not attempted here. However, this empirical study reveals many aspects of parallel behaviour of EHD with and without heat transfer, such as pressure drop variations with voltage. Since important conclusions can be drawn from the study of experimental evidence, this is now presented.

4. EXPERIMENTAL RESULTS

4.1. *The experimental apparatus*

An experimental facility, capable of testing EHD effects in laminar flow, consisting of a tube of 25.4 mm i.d. and 1 m long, was built. The device was used to test isothermal and heat transfer conditions, for which the outer surface was heated allowing saturated steam to condense onto it at near-atmospheric pressure. Shell Diala Oil 'B' was selected as the sole test fluid since its exaggerated temperature-dependent viscosity allows for the testing over a large range of axial Reynolds numbers.

All the pipes and the tank linings were copper, which had proved to be very stable when in contact with this type of oil. A schematic diagram of the experimental device is shown in Fig. 2.

Table 1. Shell Diala Oil 'B' physical data

Property	Expression	Expected error (%)
ρ	$878.2-0.631\ T$	2.5
γ	$38.3\times10^{-4}\ T^{-1.5}$	0.5
k	$0.1338-4\times10^{-5}\ T$	1.5
c_p	$1.775-0.0025\ T$	2
b	$3.41\times10^{-10}\ T^{1.505}$	2.5

The electrode itself was tensioned between its extremes and insulated with PVC sleeving at all points except at the test section itself. A voltage was supplied via a stabilized d.c. source (Brandenburg Model 807R, 0–30 000 V), connected to the electrode via a series of resistors designed to limit the current to a maximum of 100 μA.

Continuous and careful calibration ensured that errors in experimental measurements were kept within the following values: for temperatures, 0.5°C; for mass flow rate, 5% at smaller values (0.06 kg s^{-1}) decreasing to 1.5% at higher flows (>0.15 kg s^{-1}); for pressure drop, 7.5–2.5% for the limits quoted for mass flow rate; heat flux, 5–3.5% for the same limits. The condensate flow rate exhibited maximum errors of about 3%, hence the heat transfer coefficient was taken to be exact within 7–4% error for the indicated limits. Further, the repeatability of the results was tested over a period of several months, and it was found that the isothermal pressure drop in the absence of an electric field was always reproduced within 2.5%.

Direct measurement of Shell Diala Oil 'B' physical properties, together with various technical data sources on ion mobility, led to the expressions in Table 1, written as a function of temperature T (°C).

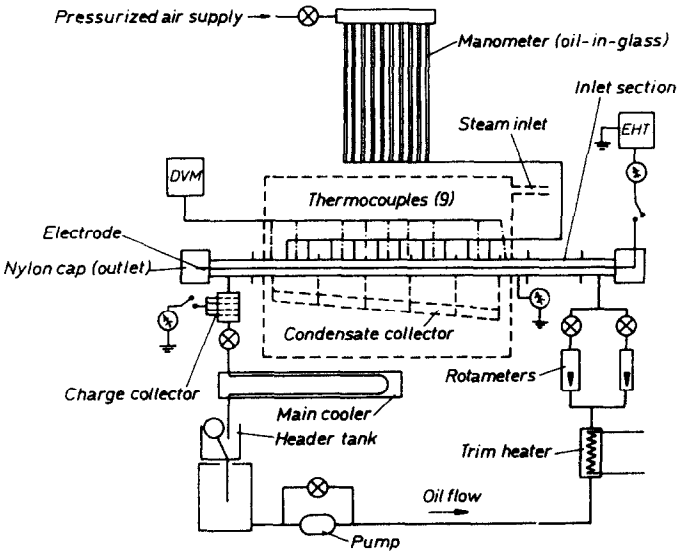

FIG. 2. Layout of heat transfer apparatus (in the isothermal apparatus, the steam jacket and condensate collector, shown dotted, were omitted).

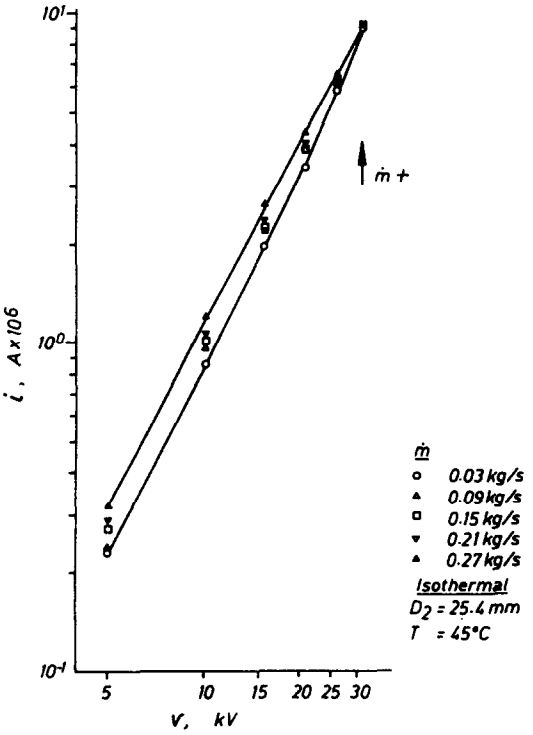

FIG. 3. Current–voltage characteristics for $T = 45°C$.

4.2. *Isothermal results*

Since current flow depends on applied voltage, the current–voltage characteristic was analysed in isothermal laminar flow. A sample of the data is shown in Fig. 3, where an increase in mass flow rate $\dot{m}$ appears to result in slight increases in current i for a fixed voltage v. Other tests revealed that current dependence on $\dot{m}$ was not consistent, but it was found that, in general, current levels behaved fairly well as $i = v^n \times$ constant, where n takes values of 2–2.25.

The action of an electric field in increasing the axial isothermal pressure drop is illustrated in Fig. 4; similar results were obtained for other oil inlet temperatures. Values along the axis of the ordinates ($i = 0$) correspond to the Hagen–Poiseuille situation ($v = 0$). In general, as the current was increased, the axial pressure gradient was seen to rise. It was noticed in all cases that for $Re < 500$ the increase in pressure drop was proportional to the current. For higher values of Reynolds number, it was seen that an initial small current had a sudden and marked effect on the pressure gradient; however, for a current larger than 2 μA, the dependence was again almost linear. This overall behaviour supported the belief that (a) the effect of electroconvection in tubes is current dependent, (b) there is no saturation effect since pressure

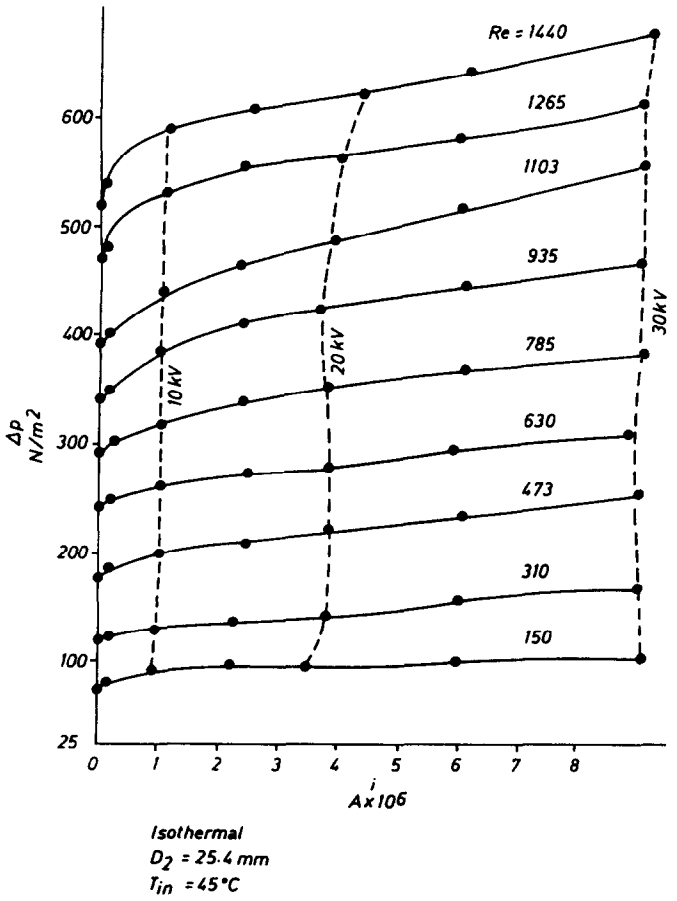

FIG. 4. Pressure drop vs current, $T = 45°C$.

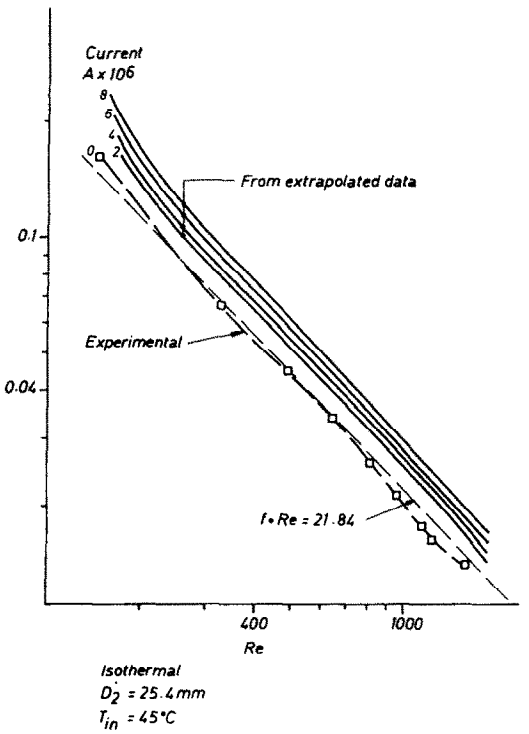

FIG. 5. Friction factor/Reynolds number characteristic for various currents, $T_{in} = 45°C$.

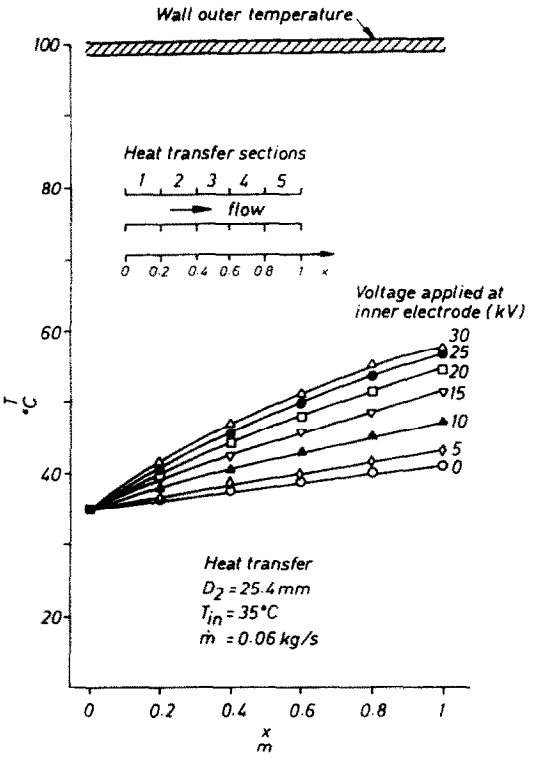

FIG. 6. Oil temperature at the outlet of the individual heat transfer sections (experimental).

drop increases with current continually until electrical breakdown, and (c) the charge/neutrals mechanism of interaction is of viscous nature, since a reduction in viscosity results both in higher current levels and in larger increases in pressure drop.

Data in Fig. 4, as well as additional data for other temperatures, allowed for the cross-plotting of pressure drop at integer values of current. A plot of friction factor (f) vs Re can thus be made, as Fig. 5 illustrates, for various current levels. The most important characteristic to observe is that the friction factor was essentially parallel to that for a non-electric flow, leading to the conclusion that when an electric field was applied, the flow retained its basic laminar nature. This result suggests that the electric field induces a well-ordered secondary motion on the axial laminar flow, a fact that implies that large increases in heat transfer are possible with relatively small increases in pumping power.

4.3. *EHD results with heat transfer*

Further tests were performed with heat transfer in the presence of an electric field. A sample of the results is shown in Fig. 6. The poor heat transfer qualities of the oil are manifest in the small temperature rise (approx. 6°C) when no electric field is applied. As the voltage rises, the outlet temperature goes up as well, until at 30 kV the outlet temperature reaches about 57°C, an increase in the overall heat transfer coefficient of about 300% in this particular case.

The overall heat transfer coefficient was obtained from measurements of steam condensate and oil temperature. Since the oil-side heat transfer coefficient was the severely limiting one, it was essentially equal to the overall coefficient. Figure 7 shows the variation of h along the tube as a function of voltage. Since the increase in oil temperature was smaller for increasing mass flow rates, the condition of constant heat flux is approached, i.e. the increase in temperature becomes approximately linear with voltage.

Figure 8 depicts the effect of applied voltage at various oil inlet temperatures. The heat transfer coefficient at the inlet stops increasing with Re at voltages of about 10 kV and decreases with Re at higher voltages until transition to turbulence is approached. The electroconvective effect is apparently the dominating heat transfer mechanism in low Reynolds number flows.

Since it has already been suggested that EHD effects are dependent on current rather than on voltage, it would be expected that heat transfer data can produce a more ordered result when plotted on this basis, as opposed to voltage. Several test runs yielded the isothermal relationship $i = f(v^n)$, which was also valid when heat transfer was imposed on the oil. From the comparison between current magnitudes with and without heat transfer, it was apparent that the current level was no longer a function of oil temperature at the inlet alone, but also of the mean oil bulk temperature and the wall temperature. A step increase of

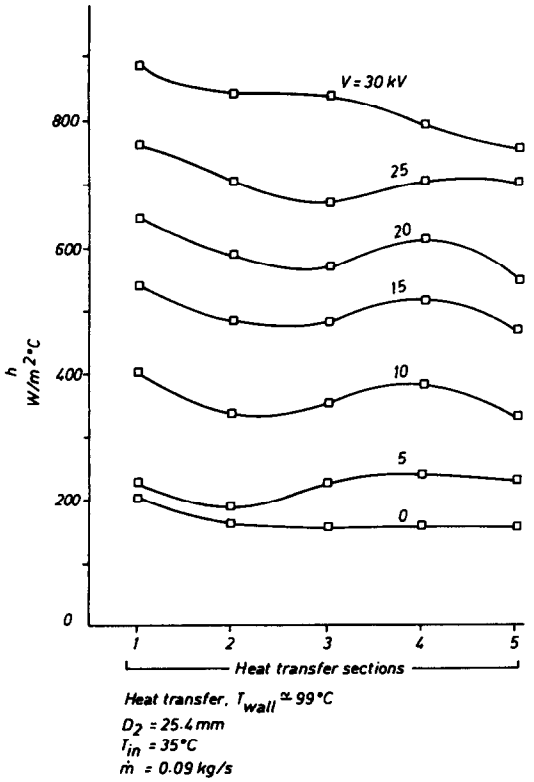

FIG. 7. Axial variation of the heat transfer coefficient for different voltages, calculated from the condensate at each heat transfer section.

10°C in oil temperature at the inlet had almost no effect on the level of current injection. Further, some mass flow rates for which an increased *Nu* was found (e.g. see $Re > 800$ in Fig. 8) correspond to higher current levels.

4.4. *Non-dimensional correlations*

The plot of *Nu* vs current level *i* shown in Fig. 9 includes data for all tests. It reveals that when electroconvection is established ($i > 1$ μA), the oil-side heat transfer coefficient is controlled by current injection alone, regardless of the value of *Re* (and therefore and most importantly, of the initial convection coefficient). Comparing data for various inlet temperatures it was found that the characteristic $Nu(i)$ relationship was maintained.

The results so far reported correspond to a maximum heat transfer increase of 500%. In order to attain higher electric field strengths the outside diameter was reduced from 25.4 to 19.05 mm. Maintaining the electrode size, the value of λ was changed from 16 to 12. A more intense electroconvective motion was obtained, corresponding to higher current levels. However, a more pronounced scattering of data was also evident. Although the behaviour illustrated in Figs. 8 and 9 was also present, the correlation could not be readily confirmed.

Results were obtained with positive and negative polarity, see Fig. 10. A negatively-charged electrode yielded, as expected, higher current levels and there-

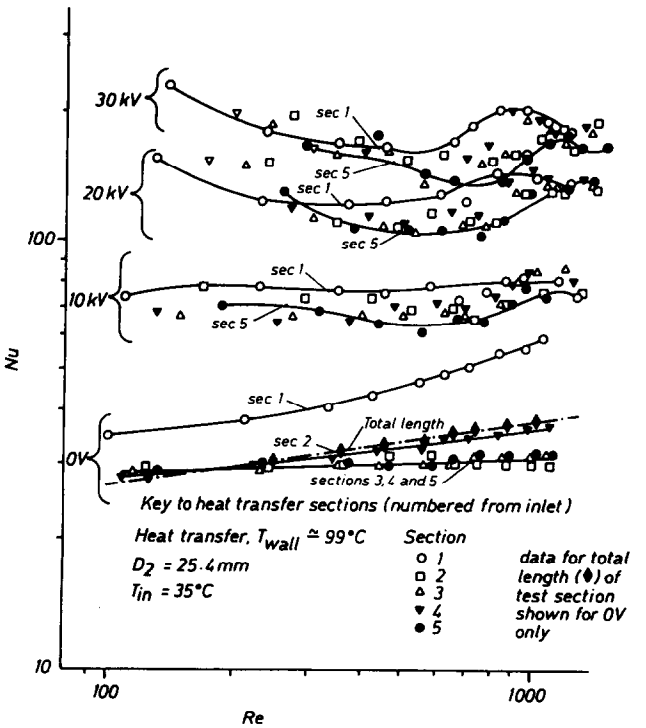

FIG. 8. Nusselt number/Reynolds number characteristics for variations in applied voltage in steps of 10 kV. Data shown for the individual heat transfer sections.

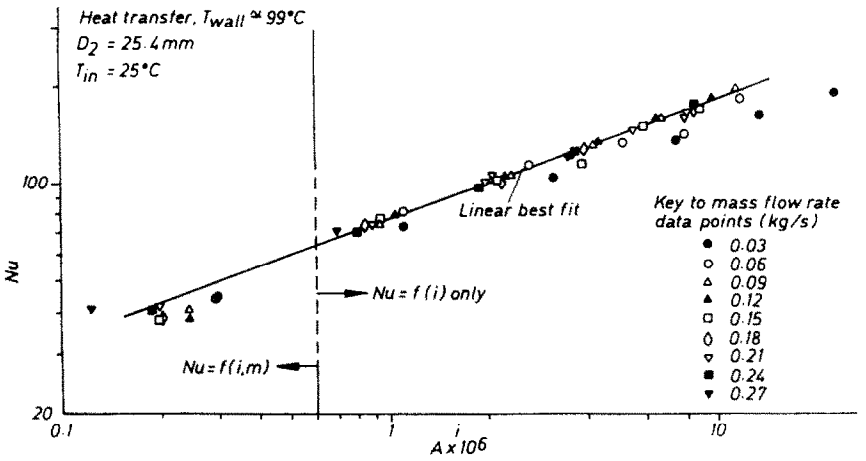

FIG. 9. Correlation of Nusselt number with current for all mass flow rates at $T_{in} = 25°C$.

fore higher enhancement rates. In this smaller tube, heat transfer enhancement rates reached the impressive level of more than 2000%.

5. EHD INCREASES IN AXIAL PRESSURE DROP

Since the effect of the electric field in promoting heat transfer was found to be independent of the flow throughput, it was concluded that the mechanism responsible for the heat transfer increases was one of convection in the radial direction, proportional to the rate of transport of electric charge. This implied that some connection must exist between the isothermal increase in pressure drop and the heat transfer intensification, as an extended Reynolds analogy would suggest. All experimental data supported the belief that increases in pressure drop were similar with and without heat transfer. Data for the smaller tube diameter supported the conclusion that small geometries resulted in a more marked EHD circulation.

Based on the examination of the experimental evidence produced this far, it is proposed that a fixed applied electric field will result in an increased axial pressure drop, under heat transfer conditions, proportional to that for flow under isothermal conditions provided that the isothermal temperature is given by

$$T_{\text{isothermal}} = (1/2)(T_{\text{in}} + T_{\text{out}})_{\text{heat transfer}} \times \left(\frac{\mu_b}{\mu_s}\right)_{F=0}^{0.14}.$$

This temperature could be used for a wide range of oil flow rates. With the data reported in the preceding sections, the larger diameter tube with an inlet temperature of 35°C results in an equivalent oil temperature for a medium oil flow rate of about 45°C. Isothermal data of Figs. 4 and 5 were used to plot Fig. 11.

Other tests confirm that pressure drop increase (with and without heat transfer) is essentially linear with current. This supports the belief that EHD effects in both cases are similar. It was noticed that lines of constant mass flow rate were essentially straight and that a change in slope occurred when the injected current exceeded 1 μA, i.e. when electroconvection was established (Fig. 12). Results with the smaller geometry confirmed that the pressure drop increase, expressed in non-dimensional form with respect to pressure drop for zero current, is entirely current dependent, regardless of voltage applied and of polarity (Fig. 13).

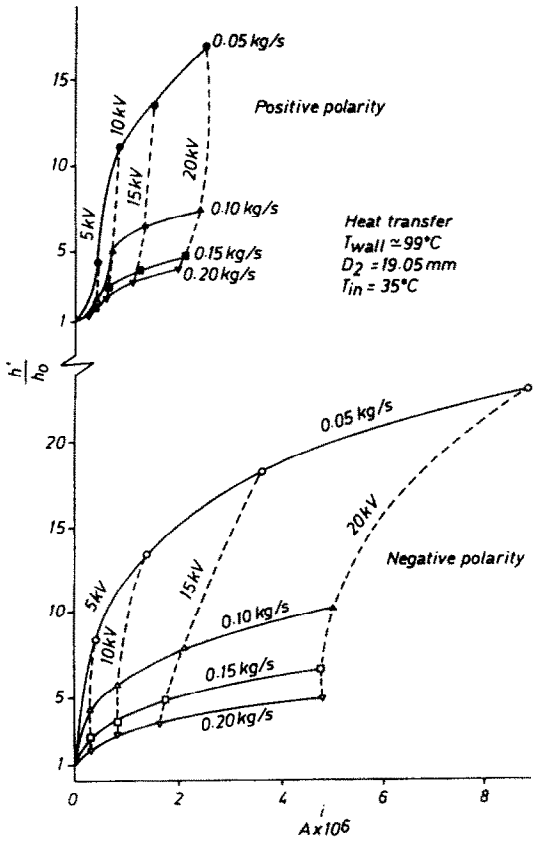

FIG. 10. Non-dimensional heat transfer coefficient vs current flow, positive and negative polarity, for various mass flow rates, $D_2 = 19.05$ mm, $T_{in} = 35°C$.

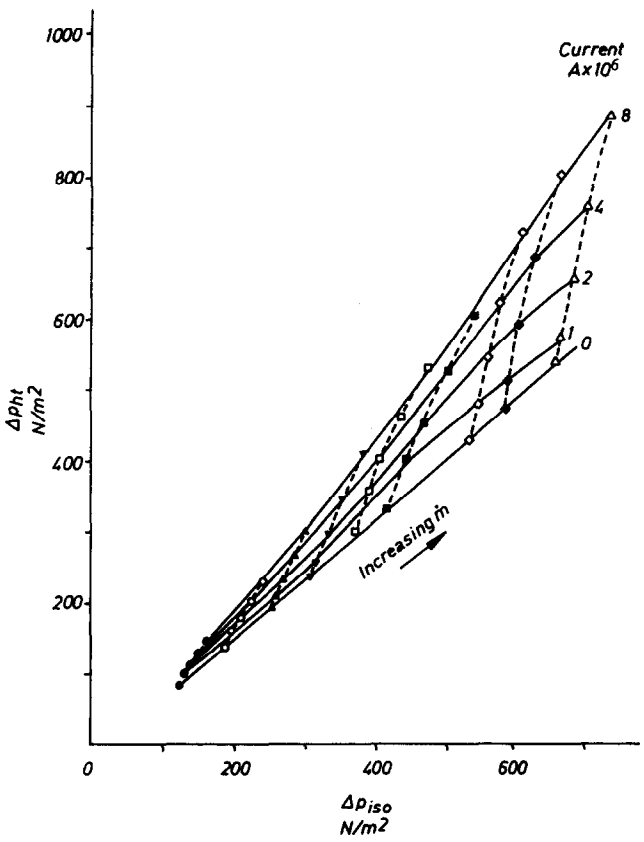

FIG. 11. Relationship between isothermal and heat transfer pressure drops for $D_2 = 25.4$ mm, based on an equivalent $T_{in} = 45°C$. Experimental data for zero current; curves for $i > 0$ plotted with interpolated data.

6. CORRELATION OF RESULTS

A correlation was attempted between these experimental data and the theoretical basis of Section 3. The one-dimensional model was shown to be equivalent to the EHD effect in respect of radial momentum flux, and the increase in axial pressure drop was related to a complex quantity α referred to as the 'radial Reynolds number', shown in equation (8). With the pertinent numerical values of the oil employed, a value for α is found in terms of the applied voltage v, the isothermal temperature T and a function of θ that is referred to as c. The value of c is at this point difficult to calculate and is evaluated empirically, since there is not enough information on $f(\theta)$ as employed in equation (4). Based upon examination of the experimental data and through successive approximations, an evaluation of c can be made. This (totally empirical) value of c results in a correct prediction of the magnitude of the pressure drop for all voltages and allows the proposed model to display the correct dynamic behaviour, as Fig. 14 depicts. The same agreement between model and experimental results is found at other oil inlet temperatures and with the smaller geometry. It must be noticed that the current dependence of the EHD phenomenon is already incorporated in the model, predicting adequate pressure drop increases for variable voltage.

7. CONCLUSIONS

EHD convection enhancement is shown to yield up to 2000% increases in heat flow rates when applied to high Prandtl number dielectric liquids, and seems therefore superior to many other systems of intensification of heat transport. Corresponding increases in pressure drop are one order of magnitude smaller. All data indicate that the same well-behaved secondary flow, viscous-type mechanism is operational with dielectric liquids within the range of $20 < Pr < 2000$ in concentric-annular geometries.

It was observed that the radial flow of charged species induces a leaf-pattern motion with a strong velocity outwards and a sluggish return flow, resulting in a finite flow of radial momentum outwards. This effect causes a distortion of the laminar axial flow, as well as an effective mixing, resulting in a measurable increase in pressure drop. Still, friction factor vs Reynolds number data for the electric field, with and without heat transfer, show that the flow retains its laminar character.

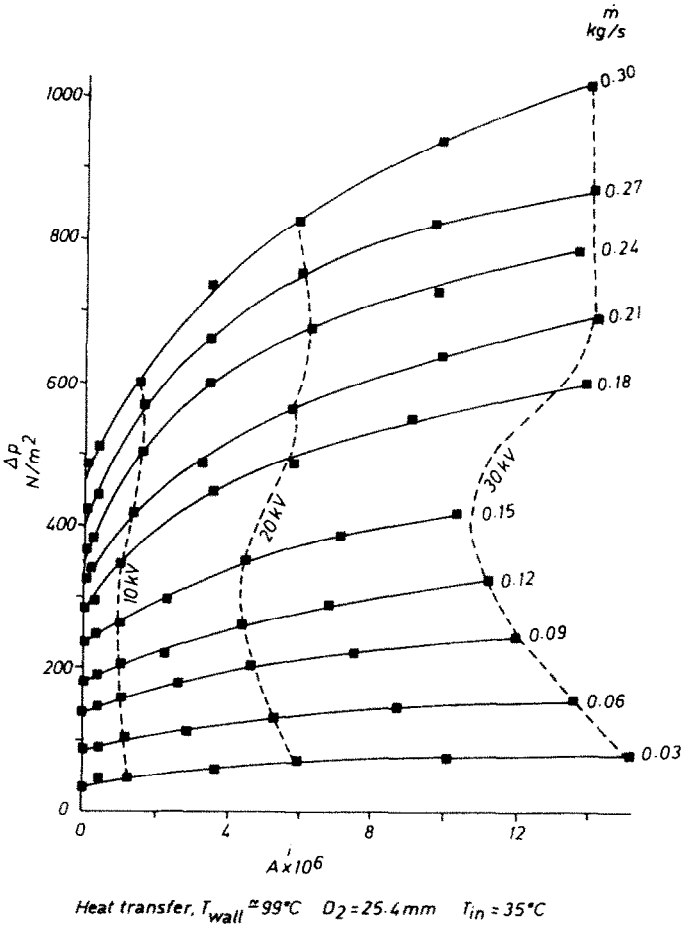

FIG. 12. Pressure drop variation with current flow for various mass flow rates, $D_2 = 25.4$ mm, $T_{in} = 35°C$.

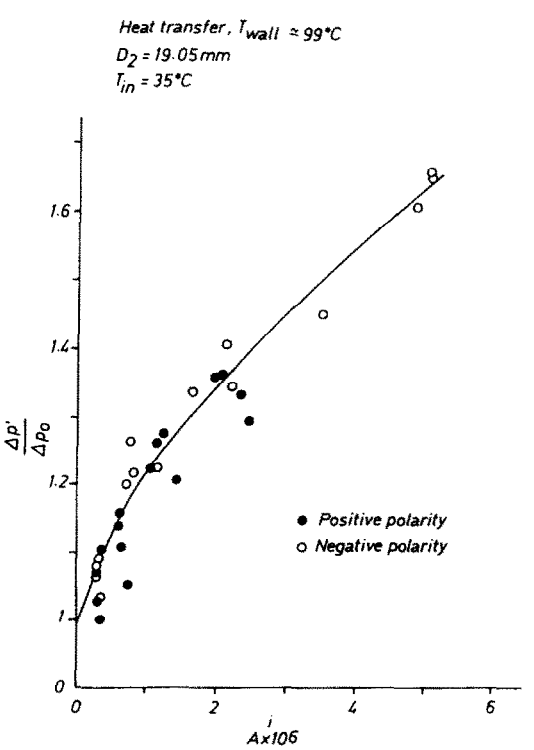

FIG. 13. Non-dimensional pressure drop vs current for positive and negative polarity, all mass flow rates, $D_2 = 19.05$ mm, $T_{in} = 35°C$.

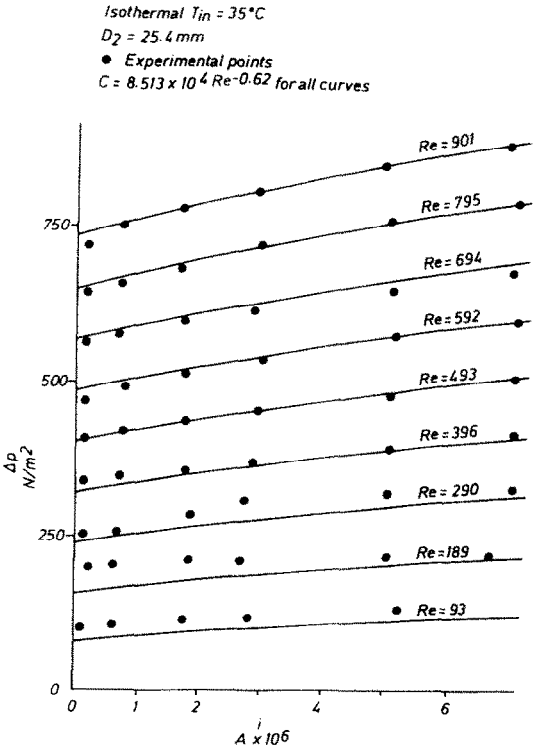

FIG. 14. Pressure drop prediction as a function of current flow (solid lines) compared with experimental data for $T_{in} = 35°C$, $D_2 = 25.4$ mm.

Several mechanisms of interaction are seen to take place simultaneously as a high voltage is applied to the central electrode (liquid heating). At the inlet, the electrode is surrounded by cold fluid so the high viscosity impedes a high electric interaction. As the oil flows downstream and is heated, the electric motions increase and dominate the heat transfer mechanism until the oil-to-wall temperature difference is so diminished that the rate of heat transport is noticeably reduced. However, the fall in viscosity also represents an increase in Reynolds number more marked than in the absence of an electric field. These effects, as it has been observed, can combine so that Nu in EHD-dominated flows is basically independent of Re.

The field is found to have an essentially electrophoretic effect on the fluid, more marked at low axial flow rates. An increase in liquid temperature resulted always in higher current levels and hence in a higher EHD effect. All effects were dependent on current level and independent of polarity. However, a negative electrode produced higher rates of charge injection than a positive one, at constant voltage.

The correlation of the experimental pressure drop data with heat transfer, and that of 'equivalent temperature' isothermal flow, reveals that a prediction of EHD is possible. A more general form of correlation is needed if the prediction of isothermal pressure drop, based on the model proposed here, is to be used for establishing design criteria. Although a single scaling factor c can be envisioned to perform this task, it must be noticed that the dependence of c implies that, whilst the nature of the variation of the 'equivalent line source' strength with applied voltage is governed by the model equation, its absolute strength is moderated by the axial flow rate.

REFERENCES

1. R. Poulter and A. T. Richardson, Electrohydrodynamic enhancement of heat transfer with single phase dielectric fluids in tubes, Aero. Res. Council Report ARC 36 395/HMT 392, London (1975).
2. R. Poulter and I. A. Miller, Heat transfer enhancement in shell/tube heat exchangers employing electrostatic fields, *Proc. 1st U.K. National Heat Transfer Conf.*, Leeds, Vol. 2, pp. 707–716 (1984).
3. R. Poulter and P. H. G. Allen, Electrohydrodynamically augmented heat and mass transfer in the shell/tube heat exchanger, *Proc. 8th Int. Heat Transfer Conf.*, San Francisco, California, Vol. 6, pp. 2963–2968 (1986).
4. A. T. Richardson, Non-linear stability bounds in electrohydrodynamics, *J. Electrostatics* **15**, 343–349 (1984).
5. A. T. Richardson and R. Poulter, Electrophoretic instability in a diffusion-free dielectric liquid in an annular geometry, *J. Phys. D: Appl. Phys.* **9**, L45–L48 (1976).
6. I. M. Williams, A. T. Richardson and R. Poulter, The origins of conduction in hydrocarbons, *Proc. 6th Int. Conf. Conduction/Breakdown in Dielectric Liquids*, Mont-St. Aignan, France, pp. 49–55 (1978).
7. P. J. Martin and A. T. Richardson, Conductivity models of electrothermal convection in a plane layer of dielectric liquid, *ASME J. Heat Transfer* **106**, 131–136 (1984).
8. R. A. Moss and J. Grey, *Proc. Heat Transfer and Fluid Mech. Inst.*, pp. 210–235. Stanford University Press, California (1966).
9. P. Atten and R. Moreau, Stabilité électrohydrodynamique des liquides isolants soumis à une injection unipolaire, *J. Méc.* **11**, 471–520 (1972).
10. P. Atten and J. C. Lacroix, Non-linear hydrodynamic stability of liquids subjected to unipolar injection, *J. Méc.* **18**, 469–510 (1979).

FLUX RADIAL DE MASSE DANS LA CONVECTION FORCEE DANS LES TUBES ET AUGMENTEE ELECTRODYNAMIQUEMENT

Résumé—Des résultats expérimentaux sont présentés pour un réchauffeur d'huile, à section annulaire, avec promoteur électrodynamique. Quand un courant continu à haute tension (30 kV) est appliqué à travers l'espace annulaire, il induit un très fort mouvement radial du fluide provoquant un accroissement de transfert thermique de plus de 20 fois celui de l'écoulement laminaire établi, alors que la perte de charge est seulement multipliée par trois. Le nombre de Nusselt de l'accroissement électrodynamique est bien relié au courant électrique qui passe, lequel est typiquement quelques millions d'Ampères par mètre de tube.

RADIALER MASSENSTROM IN ROHREN BEI ELEKTROHYDRODYNAMISCH VERSTÄRKTER ERZWUNGENER KONVEKTION

Zusammenfassung—Es werden experimentelle Ergebnisse für einen elektrohydrodynamisch verstärkten Ölerhitzer mit ringförmigem Querschnitt dargestellt. Über dem ringförmigen Spalt wurde eine hohe Gleichspannung (etwa 30 kV) angelegt, die eine sehr starke radiale Bewegung des Fluids erzeugt. Dies ergibt eine mehr als 20fache Erhöhung des Wärmeübergangs gegenüber der vollentwickelten laminaren Strömung, wobei der Druckverlust nur um das 3fache steigt. Die elektrohydrodynamisch erhöhte Nusselt-Zahl korreliert gut mit dem durchfließenden elektrischen Strom, welcher typischerweise einige Millionstel Ampere pro Meter Rohr beträgt.

РАДИАЛЬНЫЙ ПОТОК МАССЫ ПРИ ЭЛЕКТРОГИДРОДИНАМИЧЕСКОЙ ИНТЕНСИФИКАЦИИ ВЫНУЖДЕННОГО ТЕПЛООБМЕНА В ТРУБАХ

Аннотация—Приводятся результаты экспериментального исследования масляного нагревателя кольцевого поперечного сечения с электрогидродинамической интенсификацией, Подача высоковольтного (порядка 30 кв) постоянного напряжения в кольцевой зазор вызывает интенсивное радиальное движение жидкости и тем самым более чем 20-кратное усиление теплообмена в случае полностью развитого ламинарного потока. При этом перепад давления увеличивается в 3 раза. Число Нуссельта при электродинамической интенсификации хорошо коррелирует с величиной проходящего электрического тока, обычно составляющего несколько миллионных долей ампера/погонный метр трубы.